113

umma university
Fostering knowledge and Innovation

P. O. Box 713—01100 KAJIADO, KENYA TEL: 0739 969020, 0739 969021
Website: http://www.umma.ac.ke Email: vc@umma.ac.ke

REF: UU/AC/ROI/VOL.3/24 6th November 2018

Dear Sir/Madam,

RE: INVITATION TO AN INTERNATIONAL CONFERENCE ON SCIENCE, TECHNOLOGY AND INNOVATION FOR SUSTAINABLE DEVELOPMENT IN DRYLAND ENVIRONMENTS

Umma University in Kajiado County, South Eastern Kenya University (SEKU) in Kitui County, Lukenya University in Makueni County and Machakos University in Machakos County, together with other partners, are jointly organizing an international Conference entitled *"Science, Technology and Innovation for Sustainable Development in Dryland Environments"* to be held on 19th-23rd November 2018. The theme of the conference is *"Harnessing Dryland Natural Resources for Sustainable Livelihoods in the Era of Climate Change*". The conference will be two-phased with a two day pre-conference training workshop on 19th-20th November 2018 at SEKU and the main conference on 21st-23rd November 2018 at Umma University. The conference will provide an excellent platform for the academia from around the world to engage with the industry, innovators, policy makers, value chain developers, farmers, and service providers among others so that higher education in Africa contributes to solving the problems of natural resources governance in the era of climate change.

We are therefore pleased to invite you to attend the pre-conference training workshop at SEKU Main Campus in Kitui on 19th-20th November 2018 and the Main conference at Umma University on 21st to 23rd November 2018. Please note that you will be responsible for your travel and accommodation arrangements and conference registration fee.

Yours Sincerely,

DR. ALI ADAN ALI
FOR THE: VICE-CHANCELLOR

A Pressure Wave Theory for a Transient Drawdown in an Unconfined Aquifer

Waswa GW[a,b*], van Tol[b], Lorentz SA[c] and Vermeulen D[b]

[a]Department of Civil Engineering, Machakos University, Machakos

[b]Institute for Groundwater Studies, University of the Free State, Bloemfontein

[c]SRK Consulting, Ltd, Pietermaritzburg

[*]E-mail: waswageorge@gmail.com

Abstract

Previous observations indicate that when an unconfined aquifer is pumped at a constant rate, the drawdown-time curve exhibits a three-segment graph; a steep early time segment, a flatter intermediate segment and a somehow steeper late time segment. Previous studies have reported that using type curves developed from the existing analytical models, for prediction of a transient drawdown in unconfined aquifer during pumping, give unrealistically low values of specific yield. The existing analytical models were developed on the assumptions that the steep early time segment of the time-drawdown is due to the elasticity of the aquifer and water, and that the water table is a material boundary. On the contrary, previous field observations have reported that the steep early time segment of the drawdown-time curve corresponds with the period of increasing hydraulic gradients and that the water table declines more rapidly than drainage of the water from the aquifer. In this paper we present a new perspective of the physical processes and a new pressure wave theory that can account for the above observations, without considering the elasticity of the aquifer and water. The new theory has been developed on the basis that a water table is an energy boundary and can reproduce the entire three-segment drawdown-time graph based only on the changing energy boundary conditions at the pumping.

Keywords: groundwater, pressure-head diffusion, transient drawdown, unconfined aquifer

1. INTRODUCTION

Groundwater, in subsurface geologic aquifers, forms a significant source of water in many regions of the world, including Kenya where there are huge groundwater-aquifers in its northern-eastern and eastern regions (Sklash and Mwangi, 1991; Swarzenski and Mundorff, 1977). Characterization of an aquifer is important in the understanding of the quantities and yields of water from the aquifer. Aquifer hydraulic properties, e.g. transmissivity, storativity, and specific yield are the main physical characteristics that are of greatest importance in groundwater exploration and management. These properties are usually obtained from pumping test data. An aquifer pumping test is usually conducted by stimulating the aquifer through constant pumping in a pumping well and observing the aquifer response, via the drawdown (reduction in head at a point – e.g. a water level in observation well - caused by the

withdrawal of water from an aquifer). Analyses of observation well data from pumping test are then used to estimate the hydraulic properties of an aquifer.

When an unconfined aquifer is pumped at a constant rate, the transient-drawdown (drawdown versus time) exhibits three segments: a steep early time segment that follows the Theis (1935) confined-aquifer non-equilibrium response; a flatter intermediate segment that is less steep than that predicted by the Theis model; and a steeper late-time segment that again conforms with the Theis response. In practice, the hydraulic properties of unconfined aquifers are usually determined by analyzing pumping test data using theoretical models, common of which are the Boulton's (1963) model and the Neuman's (1972) model.

1.1. The Neuman's Delayed-Water-Table-Response Model

The Neuman's (1972) model was derived on an assumption that the water in the volume of sediments through which the water table has fallen is discharged instantaneously with the fall of the water table. Neuman argues that since the first steep segment of the transient drawdown curve follows the Theis (1935) model at early pumping times, an unconfined aquifer reacts to pumping for a short time after pumping begins, as would an artesian aquifer. Neuman explains that in this early segment gravity drainage is not immediate but water is released instantaneously from storage by compaction of the aquifer and by expansion of the water itself, similar to confined aquifer. It is considered that this instantaneous release of water accounts for the first steep segment. However, field observations by Nwankwor et al. (1992) showed that steep vertical hydraulic gradients exist, even at early time and that gravity drainage therefore would also commence near the well at a time almost coincident with the onset of pumping. Additionally, the elasticity of water and compressibility of aquifers, as processes that can account for the early time drainage (steep segment of the drawdown curve), have rarely been observed, quantified and reported in the field, which casts doubt on their physical reality. In fact, Neuman (1972) himself admitted that there is a general lack of data on the elastic storage properties of phreatic aquifers. Neuman (1972) explains that the flatter (delayed) intermediate segment, depicting the slow expansion rate of the cone of depression, is a result of replenishment of the initially fast-falling mean drawdown in the completely penetrating observation wells by the slow gravity drainage of the sediments from below the delayed-water table surrounding the observation well.

1.2. The Boulton's Delayed-Drainage Model

Contrary to Neuman's (1972) assumption, Boulton's (1954; 1963) model was derived based on an assumption of delayed drainage, that "the water bearing material through which the water table has fallen does not yield up its water immediately" – perhaps resulting into an elongated capillary fringe (zone of tension saturation). Boulton's model assumes that the delayed/flatter intermediate segment of the transient drawdown is a result of delayed drainage from above the falling/declining water table. This assumption is represented by an empirical delay coefficient (Boulton's delay index) in Boulton's model, to represent the delayed water release process.

Although the assumption of elongated capillary fringe has been confirmed in field observations (Nwankwor et al., 1992), Boulton's explanation that the delayed/flatter segment of the transient drawdown segment is a result of delayed drainage from

above the water table (also in line with the water-table replenishment assumption of the Neuman's model) might not be physically true. This is because a water table, unlike the top boundary of the capillary fringe, is not a material boundary (of course Boulton may have assumed so) to receive water drained from above. Instead, a water table is defined in terms of energy, as a locus of points along which the pressure head (potential energy per unit weight of water) is equivalent to local atmospheric pressure (Holzer, 2010). In fact, it is on the basis of this definition and distinction that a water table can be described and observed as having fallen more rapidly than the drainage of water (material), resulting into an elongated capillary fringe. The delayed drainage from above the falling water table, therefore, cannot adequately explain the delayed (flatter) intermediate segment of the transient drawdown.

It appears, therefore, that the physical processes that may account for the characteristic three-segment drawdown-time curve observed in unconfined aquifers during pumping are not yet fully understood; and the simplifying assumptions used by the existing commonly used analytical models, in order to arrive at analytical solution of the flow equation, do not adequately represent the physical processes during pumping of unconfined aquifer. Consequently, the prediction of the aquifer's hydraulic properties based on these existing analytical models, therefore, might not be accurate. This may ultimately result in the development and use of inaccurate groundwater management models and policies. The Objectives of this present paper are: (1) to present a new perspective of the physically processes that can account for all three segments of a transient drawdown curve in an unconfined aquifer when pumped at a constant rate; and (2) to present an energy-based mathematical model that can reproduce the observed three-segment transient drawdown curve.

2. THE PHYSICAL BASIS OF THE TIME-DRAWDOWN CURVE

We consider a one-dimensional system (in space) consisting of a partially penetrating well, drilled into an unconfined aquifer, as shown in Fig. 1. The energy coordinate, h_w, is oriented downwards. The space coordinate is oriented radially outwards from the screened section of the well.

Our interest is to predict the behavior of the pressure head with time at any point along the r-plane, as a result of pumping the well at a constant rate. It is worth noting that the behavior of the pressure head at any point within the aquifer (saturated porous media), including the water table/drawdown will be a function of the pressure head in the well fluid and within the screened section. The behavior of the pressure head at any point along the r-plane, will depend on the pressure head at the screened section of the well.

When pumping commences, the water level in the well will fall at a rate that is dependent on: the pumping rate, the size of the well, and; the rate of recharge of the well, which is also a function of the depth of the screened section of the well. These conditions lead to the transient and, ultimately, steady-state conditions at the screened section of the well. The condition at the screened section of the will ultimately, influence the behavior of the potential field along the r-axis/r-plane (and generally, at every point within the entire aquifer). The changing potential field in the aquifer will determine the direction and rate of flow (transmission) of water in the aquifer.

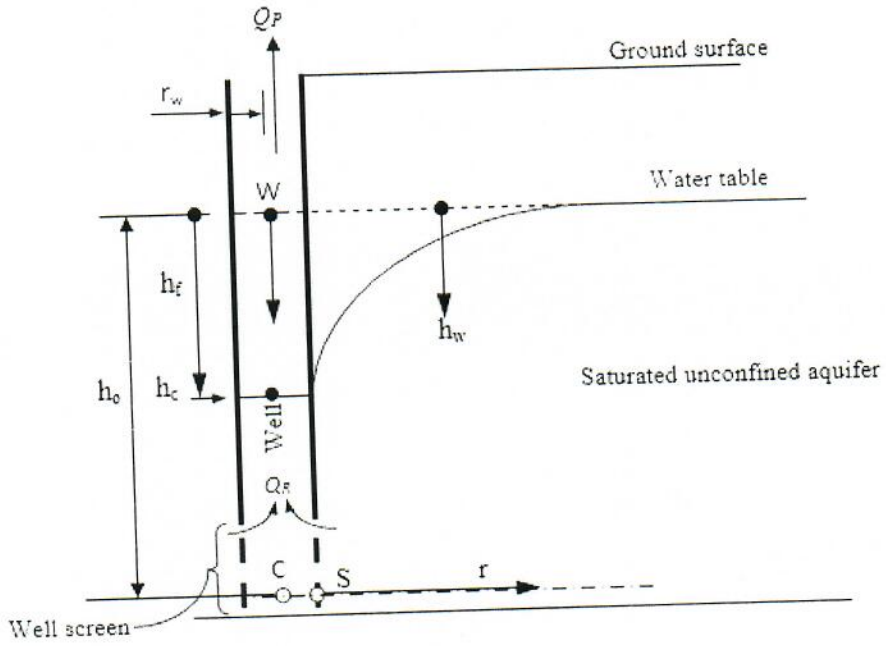

Figure 1. Idealized pumping from a well in an unconfined aquifer

3. THEORETICAL MODEL

3.1. Governing Equation

The governing equation is the new pressure wave model (Waswa and Lorentz, 2015):

$$\frac{\partial h_w}{\partial t} = d_e \frac{\partial^2 h_w}{\partial r^2} \tag{1}$$

in which, h_w is the pressure head (potential energy per unit weight of water), t is the time coordinate, r is the space coordinate and d_e is the newly introduced pressure head diffusivity coefficient (Waswa 2013) and is given as:

$$d_e = \frac{\kappa}{\rho_w g} \tag{2}$$

In which The above governing equation, Eq. (1), is solved for the appropriate initial and boundary (pressure head) conditions at the at the screened section of the well.

3.2. Initial and Boundary Conditions

The initial and boundary conditions are:

$$h_w(r,0) = h_o \quad \text{for } r \geq 0 \tag{3}$$

$$h_w(0,t) = \begin{cases} h_o - h_f & \text{for } 0 \le t \le t_c \\ h_o - h_c & t \ge t_c \end{cases} \qquad (4a,b)$$

h_c is the decreasing pressure head (varying), t is time, h_f is the final value of decreased pressure head (constant), t_c is the time that the constant decreased head conditions are achieved (constant).

It is also necessary to pose the semi-infinite boundary condition:

$$\frac{dh_w}{dr} \to 0, \qquad \text{as } r \to \infty \qquad (5)$$

3.3. Solution

The solution to Eq. (1) which can also satisfy the initial and boundary conditions Eq.s (3-5) is:

$$hw(r,t) = \begin{cases} (h_o - h_f)\operatorname{erfc}\left(\dfrac{r}{\sqrt{4d_e t}}\right) + h_o & 0 \le t \le t_c \\ (h_o - h_c)\operatorname{erfc}\left(\dfrac{r}{\sqrt{4d_e t}}\right) + h_o & t \ge t_c \end{cases} \quad \text{for} \qquad (12)$$

which is analogous to the heat conduction solution described by Carslaw and Jaeger (1959). The schematic representation of this solution is as shown in Fig. 2.

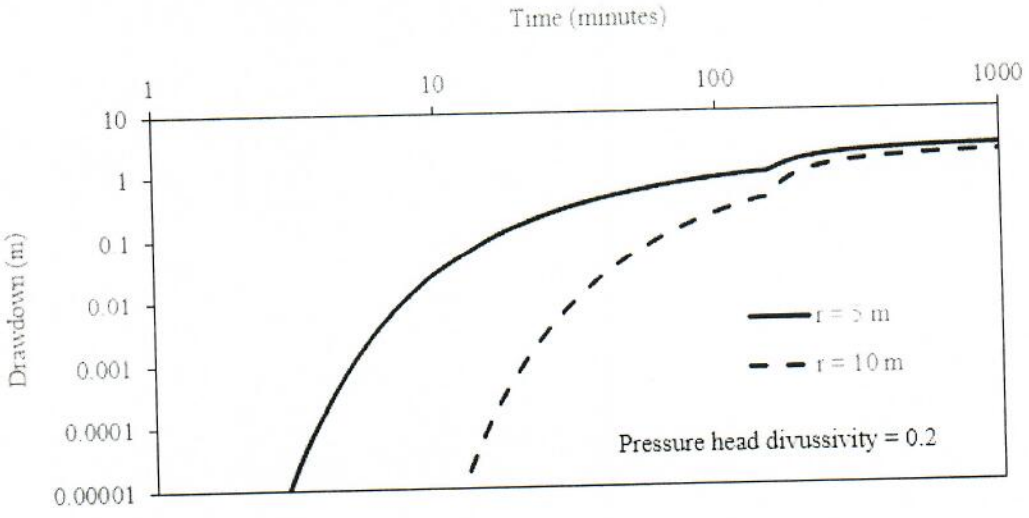

Figure 2: The log-log plot of the drawdown-transient curve based on the theoretical model

4. DISCUSSIONS

The observed time-drawdown curve is usually characterized with three segments. The mathematical model presented in this study is capable of reproducing the shape of the time-drawdown curve and indicates that the observed three-segment time-drawdown curve is as a result of the boundary conditions at the screened section of the pumping well. A combination of the boundary conditions reproduces a time-drawdown curve with three segments, similar to the one that is usually observed in the field. The first steep segment is as a result of the rapid fall in the water level in the well, when the recharge rate is still much below the pumping rate of the well. However, as pumping continues the falling rate of the well decreases because of the increasing recharge rate. This results in a decreasing falling rate of the pressure head at the screened section of the well. This is ultimately reflected in the change in gradient of the time-drawdown curve towards the horizontal (second segment). When the recharge rate equals the pumping rate, the water level in the well becomes constant; resulting in a constant pressure head condition at the screened section of the well, yielding a steeper gradient in the time-drawdown curve (the third segment).

5. CONCLUSIONS

The mathematical model presented in this study is capable of reproducing all the three segments that characterize the observed time-drawdown curve during pumping of an unconfined aquifer. The results from the mathematical model confirm the presented description of the physical processes involved in the time-drawdown curve. The three segments in the observed time-drawdown curve are as a result of the boundary conditions imposed on an aquifer at the screened section of the well. During pumping, a pressure head sink condition is created below the water table, as a result of the rapid fall of the water level in the pumping well.

It is necessary to develop relationships between parameters describing transmission of pressure head, e.g. pressure head diffusivity coefficient, and the commonly measured material parameters such as porosity (pore space), permeability (connectivity of the pore spaces), fluid density and viscosity. This is an ongoing research and ultimate results will be published later.

6. ACKNOWLEDGEMENTS

The study is funded by the German Academic Exchange Service (DAAD) and the University of the Free.

7. REFERENCES

Boulton, N. S. 1954. Unsteady radial flow to a pumped well allowing for delayed yield from storage. *Int. Assoc. Sci. Hydrol., Rome Publ.* 37, 469-477.

Boulton, N. S. 1963. Analysis of data from non-equilibrium pumping tests allowing for delayed yield from storage. Proceedings Institution Engineers 26(3), 469-482.

Carslaw, H. S. & Jaeger, J. C. 1959. *Conduction of heat in solids.* Oxford University Press: Clarendon Press. New York.

Holzer, T. L. 2010. The water table. *Ground Water* 48(2), 171-173.

Neuman, S. P. 1972. Theory of flow in unconfined aquifers considering delayed gravity response of the water table. *Water Resour. Res.* 8(4), 1031-1044.

Sklash, M. G., & Mwangi, M. P. (1991). An isotopic study of groundwater supplies in the Eastern Province of Kenya. *Journal of Hydrology*, 128(1-4), 257-275.

Swarzenski, W. V., & Mundorff, M. J. (1977). Geohydrology of North eastern province, Kenya (No. 1757-N). US Govt. Print. Off

Theis, C. V. 1935. The relation between the lowering of the piezoemtric surface and the rate and duration of discharge of a well using groundwater storage. *Transaction of American Geophysical Union* 16(1), 519-524.

Waswa, G. W. (2013). *Transient pressure waves in hillslopes* (Doctoral dissertation, University of KwaZulu-Natal, Durban).

Waswa, G. W., & Lorentz, S. A. (2015a). Transmission of pressure head through the zone of tension saturation in the Lisse effect phenomenon. *Hydrological Sciences Journal*, 61(10), 1770-1777.

Pressure head and groundwater flow dynamics at a wetland zone in a headwater catchment

George W Waswa[1,2,4*], Johan van Tol[1], Simon A Lorentz[3] and Danie Vermeulen[4]
1 - Department of Crop, Soil and Climate Sciences, University of the Free State, South Africa
2 - Department of Civil Engineering, Machakos University, Kenya
3 - SRK Consulting (Pty), South Africa
4 - Institute for Groundwater Studies, University of the Free State, South Africa

Abstract
This paper presents results of field observations of intense rainfall-induced downwelling and upwelling pressure heads and the analyses of their effects on groundwater flow at a wetland zone in a headwater catchment in South Africa. A transect spanning from: a steep hillslope zone, through a transition and a flat low-lying wetland zones, to a stream-channel zone; was instrumented with tensiometers to monitor the responses of pore-water energy to rainfall events. Results show that prior to the season, groundwater flow was from both the stream-channel and the steep hillslope zones, towards the transition zone where there was a water table trough. The season's early rainfall events caused the then deep water table at the wetland and channel zones to respond, but without infiltration at the latter. Localized infiltration at the wetland zone resulted in the formation of a groundwater mound in this zone and reversed the flow that recharged the groundwater beneath the stream-channel zone. The season's late rainfall events simultaneously caused the pressurized air driven Lisse effect and the capillary fringe assisted groundwater ridging water table responses at the transition and wetland zones, respectively. During the events, the Lisse effect dissipated, but followed by sequences of stepped increases in pressure head in the deep soil profile at the transition zone. These stepped increases in pressure head, whose magnitudes also increased with depth, were caused by the upwelling pressure heads induced by rainfall spike intensities at the wetland zone. These observed pressure head dynamics could have major and disproportionate influence on groundwater flow.

1. INTRODUCTION

The rate and direction of groundwater flow are a function of the gradient of the hydraulic head. Components of the hydraulic head are gravity head and pressure head. Pore-water pressure head is usually with reference to atmospheric pressure. The zone in which the pore-water pressure head is below atmospheric (negative pressure head) is referred to as the vadose zone. The zone in which the pore-water pressure head is above atmospheric (positive pressure head) is referred to as the phreatic zone. The boundary between the two zones is the water table, i.e., where the pore-water pressure head is atmospheric (zero pressure head). The flow of groundwater above the water table (i.e. in the vadose zone) is usually relatively slow and mainly under the influence of capillary forces. The flow of groundwater below a water table (i.e. in the phreatic zone) is usually relatively rapid and mainly under the influence of gravitational forces. Therefore, a water table configuration and response can have a pronounced effect on the direction and rate of groundwater flow. Heliotis and DeWitt (1987) recognized three types of water table responses to rain, namely: groundwater ridging, the Lisse effect, and the storage type due to rain infiltration and recharge of groundwater.

Groundwater ridging is the rapid water table response to a rainfall event, in an environment where, in the pre-event period, a capillary fringe extends to or intersects the ground surface (Miyazaki et al., 2012). Gillham (1984) was among the first researchers to explain the physical processes involved in this phenomenon. Based on the Young-Laplace concept of capillarity, Gillham (1984) explained that an addition of a very small amount of water at the ground surface fills the capillary meniscus and relieves the capillary tension, resulting in an almost instantaneous rise of the water

*George W Waswa, Email: waswageorge@gmail.com; waswagw@ufs.ac.ke; waswageorge@mksu.ac.ke

table to the ground surface. This explanation was supported by subsequent studies of laboratory experiments (e.g. Abdul and Gillham, 1984), field experiments (e.g. Novakowski and Gillham, 1984; Helliotis and DeWitt, 1987), and numerical simulations (e.g. Jayatilaka *et al.*, 1996). Furthermore, some researchers (e.g. Cloke *et al.*, 2006; Zang *et al.*, 2017) attempted to describe the phenomenon using mass balance equations. However, it is worth noting that in the capillary fringe, which is also descriptively referred to as the zone of *tension saturation*, every pore is fully occupied with water (*saturated*) whose pressure head is below atmospheric pressure (in *tension*). In terms of energy, therefore, the capillary fringe is part, and at the bottom, of the vadose zone. A water table, which is the boundary between the vadose zone and phreatic zone, is also defined in terms of energy as the locus of points along which pressure head is zero (Holzer, 2010). Therefore, the difference between the capillary fringe and the phreatic zone is only in the energy content, otherwise both zones are ideally saturated. It follows that the conversion of the capillary fringe into phreatic (zone) water requires only an addition of pressure head (energy), a process that will automatically elevate the water table, not necessarily to the ground surface but, to a position that will depend on the amount of energy added. Certainly, results of field observations of groundwater ridging in the Weatherley Research Catchment in South Africa (Waswa *et al.*, 2012) and other study sites (Waswa and Lorentz, 2015b) indicated a direct relationship between the intensity of rainfall and the water table rise.

The Lisse effect is the rapid response of a water table due to pressurized pore air ahead of a wetting front. Freeze and Cherry (1979) explained that in the Lisse effect, the compressed pore air pressure acts directly on the water table, resulting in an equivalent rise in the groundwater level in a well. Weeks (2002) considered the Lisse effect, and the associated water table, as a material phenomenon, and explained that the pressurized air pushes the water from the aquifer into the well to produce a water-level rise to compensate for the pressure difference between the confined air pressure and the atmospheric pressure; and that a minor drawdown of the water table may be induced as water flows from the aquifer into the well as its water level rises. However, recent laboratory and theoretical investigations (by Waswa *et al.*, 2013; Waswa and Lorentz, 2015a) revealed that the Lisse effect is an energy phenomenon, in that the rapidly pressurized pore air induces an additional pressure head into the aquifer, resulting in a rapid rise of the water table that is properly indicated by the rapid rise of the water level in an observation well (McWhorter and Sunada, 1977).

Localised water table responses might results in changes in the water table configuration and, hence, changes in the rate and/or direction of groundwater flow. Gillham (1984) gave some hypothetical field illustrations of how the groundwater ridging rapid water table response, in an undulating topography, might promote a highly transient and complex groundwater flow such as the rapid delivery of pre-event groundwater into a nearby stream channel and unexpected reverse flow into a hillslope. Novakowski and Gilham (1988) used simulated rainfall experiments on a field plot to demonstrate that under shallow water table conditions, the presence of the capillary fringe can induce a rapid and disproportionate response to precipitation and that in areas of rolling and undulating topography a disproportionate water table response can result in highly transient and complex hydraulic head distributions. Abdul and Gilham (1984) used a laboratory physical model to demonstrate that the rapid rise of the water table in groundwater ridging phenomenon can result in the rapid delivery of pre-event groundwater into a nearby stream channel. More recently, Zang *et al.* (2017) used a numerical two (water-air) phase flow mass balance model to demonstrate that Lisse effect pressurized airflow in the upslope mitigates the dissipation of groundwater ridging into a hillslope. They also demonstrated that groundwater ridging can also be observed where an unsaturated zone is above the capillary fringe with a subsurface lateral flow.

From the above review, it appears that the effect of rapid groundwater table responses on local groundwater flow and under natural rainfall has not been studied. The objective of this paper,

therefore, is to present field observations of rapid groundwater table responses to natural rainfall events and their effect on local groundwater flows.

2. MATERIALS AND METHODS

2.1 Study Area

Field observations were carried out in the Weatherley research catchment, located in the uMzimvubu Water Management Area in the northern Eastern Cape Province in South Africa (Figure 1). The catchment, which covers 1.5 km^2, is located at 31° 06' 00" South, 28° 20' 10" East and approximately 1300 m above mean sea level.

The catchment drains in a northerly direction and the contributing hillslopes are generally steep. Wetland conditions, which seasonally expands and contracts, exist along the entire reach of the stream. The Mean Annual Precipitation is 740 mm, of which over 70% is concentrated in the summer months of November to March.

The land cover at Weatherley is predominantly Highlands Sourveld grassland, and typical grass species include *Themeda triandra* and *Tristachya leucothrix*. Succulent species of the genera *Aloe* and *Crassula* are also common on shallow slopes.

The soils at the catchment display a varying degree of wetness and colour and include red and yellow apedal mesotrophic soils as well as neocutanic and hydromorphic soils. The western slope of the catchment, from where the results presented in this study were obtained, is dominated by brown to dark reddish brown Huuton form with sandy loam soils at the surface and sandy clay loam subsurface soil. The Clovelly form is also encountered with bleached loamy sand and sandy loam top soils on brown sandy loam subsoil. Laboratory tests of hydraulic properties of the soils near the wetland zone indicated values of pore air entry pressure head of about 45 cm-H_2O and saturated hydraulic conductivity of between 2.35 and 11.32 cm/h (Waswa *et al.*, 2012; Waswa 2013).

2.2 Experimental Set-Up

The research catchment was established in 1995 with the aim of assessing the impact of afforestation on water resources. Afforestation of the catchment, however, was done in January 2002 (Lorentz *et al.*, 2001).

The catchment was divided into two sub-catchments, the upper sub-catchment (in the south) and the lower sub-catchment (in the north). The stream channel was installed with two weirs to gauge the flows from each sub-catchment. Full weather stations are located near the upper and lower weirs and there is an additional tipping bucket rain gauge on the crest of the eastern hillslope in the north-eastern corner of the catchment. Each sub-catchment was installed with a transect of observation nests (Figure 1) that consisted of instruments to monitor shallow groundwater levels and pore-water pressure heads.

The results reported in this paper are from sub-transect of some of the observation nests in the upper sub-catchment; namely: U1, U2, U3 and U4, which represent four hillslope zones: the steep hillslope zone, the transition zone (from steep to flat), the low lying flat zone (also called the wetland zone) and the stream-channel zone. Each of the four observation nests was installed with two or three ceramic cup tensiometers, in a vertical alignment and at depths indicated in Figure 2. Observations of the responses reported in this study are of some representative rainfall events that occurred during the summer season of 2000/2001 (September 2000 to April 2001).

2.3 Rainfall Events

Ninety-six rainfall events were recorded in the catchment during the 2000/2001 summer season (Waswa *et al.*, 2012; Waswa, 2013). Five representative rainfall events, Events 2, 3, 70, 75 and 76, will be used in this paper. Event 2 and 3 represent the season's early rainfall events and Events 70, 75 and 76 represent the season's late rainfall events. These events, whose characteristics are summarised in Table 1, were selected in order to understand the responses of the catchment in those two parts of the season. Generally, the season's late rainfall events were heavy and with spike intensities, and occurred when the soil profile at the study site was pretty wet.

3. RESULTS AND DISCUSSIONS

3.1 Infiltration and Groundwater Recharge

The responses of the pore-water pressure head to rainfall Events 2 and 3 are presented in Figure 3. Prior to the rainfall Event 2, the pore-water pressure heads at the shallower depths at U2 and U3 were significantly negative (in tension/suction), indicating that the soil profiles at these nests were in very dry conditions and the water table was deep. For instance, at U3, prior to the rainfall Event 2, the pressure heads at 20 cm and 100 cm depths were -110 cm-H_2O and -10 cm H_2O, respectively. Assuming a profile of uniform soil, whose value of pore air entry pressure head was -45 cm-H_2O (Waswa *et al.*, 2013), these observed results indicate that the water table was at 110 cm below ground surface and the unsaturated zone extended to 65 cm from the ground surface. Similar conditions existed at U2.

At U4, prior to rainfall Event 2, the pressure head at 30 cm and 100 cm depths were 30 cm-H_2O and 20 cm-H_2O, respectively. These results indicate the presence of two phreatic zones and water tables at this nest, that is: perched water table above the 30 cm depth and another deep water table at 20 cm above 100 cm depth (80 cm below ground surface). A laboratory test of the soil from this nest (by Lorentz *et al.*, 2001) indicated the presence of clay soil. The perched water table, therefore, could be a result of some lenses of clay. The two phreatic zones were separated by vadose (unsaturated zone) conditions.

With the above prior conditions, the pressure heads at all depths at U2 and U4 did not respond to the rainfall Event 2. The unresponsiveness of pressure head at U4 could be explained by the presence of the clay loamy soil which does not easily allow infiltration and recharge. The unresponsiveness of the pressure heads at U2 could be due to the steep terrain of the site which did not allow sufficient concentration of rainfall for infiltration to take place. Additionally, rainfall Event 2 was generally of very light intensity and small amount (Table 1) to cause an appreciable infiltration of a dry soil.

Nevertheless, at U3, rainfall Event 2 caused the pressure head at 20 cm depth to increase by 60 cm-H_2O, i.e. from -110 cm-H_2O to about -50 cm-H_2O, within 10 hours. The pressure head at 100 cm depth, however, showed only a slight response. These responses indicate normal infiltration process at U3, of which the infiltrated rainfall substantially increased the water content at 20 cm depth and the wetting front did not reach the 100 cm depth. The pressure head at 20 cm depth remained nearly constant at -50 cm-H_2O for 36 hours, up to the initial period (first 2.5 hours) of the rainfall Event 3, during which the pressure head at this depth again significantly increased to around 0 cm-H_2O. During this initial period (2.5 hours) of Event 3 the response in pressure head at 100 cm depth, again, was insignificant. Similar results were observed at U2, where the pressure heads at 30 cm depth significantly increased, while the responses in pressure heads at 100 cm and 190 cm depths were generally negligible. This behaviour of the significant response in the pressure heads at shallower depths and non-responsiveness or very slight responses in deep soil profile indicate a normal infiltration process, where the wetting front does not reach the deep soil profile.

It is also worth noting that during the entire rainfall Event 3, the pressure heads at the shallow depths at U2 and U3 all increased to and remained around 0 cm-H_2O. However, at U3 the pressure head at 100 cm depth gradually increased to around 80 cm-H_2O, which indicated a gradual rise of the water table due to recharge of groundwater by the infiltrating rainwater at this nest.

3.2 Groundwater Mound and Groundwater Flow

At U4, the pressure head at 100 cm depth (deep soil profile) continuously responded throughout the rainfall Event 3 while the pressure head at 30 cm depth (shallow soil profile) did not respond at all (i.e. remained constant at around 30 cm-H_2O). These results are unexpected, and contrary to observations made at other nests, i.e. U2 and U3 where, as expected and already explained, the pressure head at shallower depths responded to rainfall events and ahead of the pressure head at deeper soil profile, clearly indicating direct infiltration process. Therefore, at U4, infiltration appears not to have taken place to account for the observed pressure head responses at 100 cm depth. A consideration of the neighbouring nests reveals that during Event 3 the pressure head at 100 cm depth at U4 responded in a similar pattern as the pressure head at 100 cm depth at U3. These results indicate that the pressure head at 100 cm depth at U4 responded to the recharge of the groundwater (at U4) from U3, in a process that is illustrated in Figure 4. The water table configurations in Figure 4 were derived from the results of pressure head responses at the respective nests and times (presented in Figure 3).

Initially, prior to rainfall Event 2, the water table (hydraulic gradient) between U4 and U3 was tilted towards U3 and, consequently, the direction of groundwater flow was from U4 to U3 as indicated in Figure 4(a).

During Event 3, due to a relatively flat terrain and a more porous sandy loamy soil at U3, infiltration at this nest was faster than at nest U4. This rapid and localized infiltration resulted in rapid recharge of the groundwater and rapid elevation of the water table at U3, forming a groundwater (table) mound at this zone (Figure 4b), which reversed the direction of flow of the groundwater towards U4. The reversed flow to U4 resulted in recharge of deep groundwater at U4 and caused the observed increase in pressure head in the deep soil profile (including 100 cm depth), without the process of direct rainfall infiltration at nest U4 (Figure 4b). Similar observations of the formation of groundwater (table) mounds and reversals of direction of flow were reported by Rosenberry and Winter (1997).

3.3 Downwelling pressure heads and Groundwater Ridging Rapid Water Table Response

Results of the pressure head responses to rainfall Events 70, and 75 and 76 are presented in Figures 5, and 6, respectively. Event 70 had 3 spike intensities (Figure 5d) and Events 75 and 76 had 4 spike intensities combined (Figure 6d). From the results in Figure 5, it can be noted that prior to Event 70, at U4, the pressure head at 30 cm and 100 cm depths were 20 cm-H_2O and 100 cm-H_2O, respectively. These indicated a single water table that was at 10 cm below ground surface and the capillary fringe (the zone of tension saturation) intersected the ground surface. At U3, prior to rainfall Event 70, the pressure heads at 20 cm depth and 100 cm depth were -10 cm-H_2O (tension/vadose conditions) and 65 cm-H_2O (phreatic conditions), respectively. Since the soil at this nest had a pore air entry pressure head value of -45 cm-H_2O these observed results indicate that the water table was at 30 cm below ground surface and the capillary fringe (zon e of tension saturation) intersected the ground surface.

It can be seen from Figure 5 that, with above prior conditions, the rainfall Event 70 caused the pressure heads at all depths at both U3 and U4 to respond simultaneously and rapidly. At U4 the

pressure head at 30 cm depth increased by about 15 cm-H_2O, while at U3 the pressure head at 20 cm depth increased by about 30 cm-H_2O, in a process that rapidly converted the capillary fringe vadose water into phreatic water and elevated the water table to the ground surface at both nests. Note that the increase in pressure heads at the shallow depths were about the same magnitude as the depth of the capillary fringe prior to the event. At both nests the pressure head at 100 cm depth responded in the same pattern as at shallow depths but the responses were translated in time and attenuated in magnitude.

Results in Figure 6 show that prior to rainfall Event 75 at U4 the pressure heads at 30 cm and 100 cm depths were 30-H_2O and 110 cm-H_2O, respectively. At U3, the pressure heads at 20 cm and 100 cm depths were 20 cm-H_2O and 95 cm-H_2O, respectively. These results indicate that at both nests the water table was already at the ground surface and the capillary fringe was absent. On these prior conditions, it can be noted that rainfall Event 75 did not cause any appreciable response in pressure heads at both U3 and U4.

A comparison of the observed results from nests U4 and U3, i.e., the initial conditions prior to the respective rainfall events (Events 2 and 3 in Figure 3, Event 70 in Figure 5 and Events 75 and 76 in Figure 6) and the responses of the pressure heads at these nests, clearly reveals the role of a capillary fringe in groundwater ridging rapid water table response.

Prior to rainfall Events 2 and 3 the water table at U3 was deep below the ground surface, and so was the capillary fringe. A very dry (unsaturated) zone existed between the ground surface and the top of the capillary fringe. On these initial conditions it was noted that the rainwater at the ground surface infiltrated and percolated down (through the empty pores in the unsaturated zone) and recharged the deep groundwater, hence causing the water table to gradually rise towards the ground surface.

Prior to rainfall Event 70, the water table at U3 was shallow (at 30 cm below ground surface) and the capillary fringe intersected the ground surface. It is worth noting here that in the capillary fringe, also known as the zone of *tension saturation*, every pore space is fully occupied (*saturated*) with water that is in *tension*. Within this definition, therefore, at U3, prior to Event 70, due to the presence and position of the capillary fringe, the ground surface was saturated with (pore) water that was in tension. On these initial conditions, it was noted that the intense rainfall at the ground surface caused a rapid response of pressure head throughout the soil profile, converted the capillary fringe into phreatic water, and raised the water table to the ground surface. Since at U3 the ground surface was already saturated, the intense rainfall could not (rapidly) infiltrate the soil profile to cause the observed rapid responses in pressure head. Note that the difference between a capillary fringe and a phreatic zone is only in the energy content, and the conversion of the former into the later requires only an additional energy. In the groundwater ridging phenomenon, the kinetic energy-laden intense rainfall induces additional pressure head into the potential energy-deficient capillary fringe (tension pore-water) at the ground surface. The induced pressure head is diffusively transmitted down (downwells) through the pore-water, elevating the pressure head at every depth of the soil profile.

Prior to Event 75, at U3, the water table was already at the ground surface and therefore the capillary fringe was absent. Results showed that an intense rainfall at the ground surface only caused a pressure pulse through the soil profile without elevating the pressure heads. Note also that in Event 70, after the water table had been elevated to ground surface by the first spike intensity, the subsequent spike intensities (no. 2 and 3) only caused pressure pulses through the soil profile without raising the pressure heads at U3. (These pressure-pulses, however, and as will be discussed in the next section, may have upwelled in the neighboured).

From the above discussion it is clear that for groundwater ridging rapid water table response to occur: first, the capillary fringe should be present and extend or intersect the ground surface. Second, there should be an intense rainfall at the ground surface. The extension of the capillary fringe to the ground surface provides the necessary contact between the kinetic energy-laden raindrops of the intense rainfall and the tension (potential energy deficient) pore-water, so that the kinetic energy from the raindrops can be rapidly induced, as additional potential energy, into the tension (potential energy deficient) pore-water. This view of the role of the capillary fringe in groundwater ridging is in agreement with those of Marui *et al.* (1997) who concluded from field studies that the rapid response of pore-water pressure observed in the deep soil profile was assisted by pressure head transmission through pore spaces occupied by a relatively continuous water phase. Therefore, for capillary fringe assisted groundwater rapid water table response to occur there should be sufficient (tension saturated or near saturated) continuous pore-water phase from the ground surface to the water table below.

3.4 Upwelling Pressure heads and the rapid deep water table responses

Results in Figure 5 show that at U2, prior to Event 70, the pressure head at 100 cm and 190 cm depth were -20 cm-H_2O and 0 cm-H_2O, respectively. This implied that the water table was at 190 cm depth below ground surface and the tensiometer at 100 cm was within the zone of tension saturation/near saturation. The first spike intensity of rainfall Event 70 caused the pressure head at both depths to simultaneously and rapidly increase, by the same magnitude, into phreatic conditions. The pressure heads at both depths then recovered uniformly up to the time of the second spike intensity, when the pressure heads at both depths suddenly increased; however, the pressure head at 190 cm depth increased more rapidly and significantly than the pressure head at 100 cm depth. The third spike intensity caused further stepped increase in pressure head at both depths, and again with the increase at 190 cm depth being higher than that at 100 cm depth. After the rainfall event, the pressure head at 190 cm depth continued to increase steadily while the pressure head at 100 cm depth recovered into vadose conditions. Similar results were recorded during Events 75 and 76.

From the results in Figure 6 it can be seen that at nest U2 and prior to Event 75, the pressure heads at 30 cm, 100 cm and 190 cm depths were -80 cm-H_2O, -10 cm-H_2O and 0 cm-H_2O, respectively. These indicated that the water table was at 190 cm depth, the capillary fringe or near saturated conditions extended just above the 100 cm depth, and the unsaturated zone extended to the ground surface. The first rainfall spike intensity caused a steep increase in pressure head at all depths, but the pressure head at 30 cm depth increased more significantly than at both 100 cm and 190 cm depths. However, just like in Event 70, the pressure heads at 100 cm and 190 cm depths (which were initially in saturated/near saturated conditions) responded and recovered uniformly up to the second rainfall spike intensity, which caused the pressure heads at both depths to increase, but 190 cm depth recording a more significant increase than the 100 cm depth. In summary, the spike intensities of rainfall Events 75 and 76 also caused stepped increases in pressure head at all depths. The pressure head at the shallower depth (at 30 cm depth), however, responded and recovered more rapidly and immediately, indicating a passing wetting front/infiltration profile. On the other hand the pressure head at 100 cm and 190 cm depth displayed a relatively delayed and slow response, but with the pressure head response at 190 cm always being higher than at 100 cm depth.

These stepped increases in pressure head at U2 (transition hillslope zone) during Events 70 and 75 can be interpreted with respect to the groundwater ridging processes at the wetland zone (nest U3). First, note that at U3, at the start of Event 70, when the water table was shallow and the capillary fringe extended to the ground surface, the pressure head at 20 cm depth responded more rapidly and to a higher magnitude than at 100 cm depth. When the water table was at the ground surface at U3, during Events 70, 75 and 76, the spike intensities caused the pressure heads in the saturated

and near saturated soil profile at U2 to respond but in an inverse manner as the capillary assisted groundwater ridging pressure head responses observed at U3 at the start of Event 70. That is, while in groundwater ridging phenomenon the pressure heads in shallower soil profile (e.g. at 30 cm depth) responded more significantly than in deep soil profile (e.g at 100 cm depth), at U2 the pressure heads in deeper soil profile (e.g. at 190 cm depth) responded more significantly than in shallower soil profile (e.g. at 100 cm depth). It should be noted that in groundwater ridging the source of pressure head is at the ground surface and the pressure head diffuses downward (downwelling) through the pore-water (Waswa et al., 2013; Waswa and Lorentz, 2015a). Inversely, at U2, it appears that the source of pressure head is from below and the pressure head diffuses upwards (upwelling) through pore-water. From this analysis, it appears that the downwelling intense-rainfall induced pressure head (pressure puklses) at the wetland zone (when the water table is at the ground surface) is upwelled as rising pressure heads at U2, thereby causing the observed elevated pressure heads and water table at U2, and as illustrated in Figure 7.

4. CONCLUSION

Localized infiltration can result in groundwater mound which can change the direction and rate of groundwater flow.

For capillary fringe assisted groundwater ridging rapid water table response to occur, a sufficient (tension saturated/near saturated) continuous water phase from the ground surface to the water table is necessary.

At the sites with undulating topography, both the Lisse effect and groundwater ridging rapid water table responses might result in an unexpected and disproportionate groundwater flow dynamics.

Intense rainfall induced pressure heads at a zone with the water table at the ground surface can be diffusively transmitted through pore-water, upwelled and elevate the pressure heads and water table in the neighbouring zone.

5. ACKNOWLEDGEMENT

This study was funded by the Germany Academic Exchange Service and the University of the Free State. Field studies were funded by the Water Research Commission of South Africa.

6. REFERENCES

Abdul AS, Gillham RW (1984) Laboratory studies of the effects of the capillary fringe on streamflow generation. *Water Resources Research* 20, No. 6: 691-698.

Cloke HL, Anderson MG, Mcdonnell JJ, Renaud JP (2006) Using numerical modelling to evaluate the capillary fringe groundwater-ridging hypothesis of streamflow generation. *Journal of Hydrology* 316, No. 1: 141-162.

Gillham RW (1984) The Capillary Fringe and its Effect on Water-Table Response. *Journal of Hydrology* 67, No. 1: 307-324.

Heliotis FD, DeWitt CB (1987) Rapid water table responses to rainfall in a northern peatland ecosystem. *Water Resources Bulletin* 23, No. 6: 1011-1016.

Holzer TL (2010) The water table. *Groundwater* 48, No. 2: 171 – 173.

Jayatilaka CJ, Gillham RW (1996) A deterministic-empirical model of the effect of the capillary fringe on near-stream area runoff. 1. Description of the model. *Journal of Hydrology* 184: 299 - 315.

Lorentz S, Thornton-Dibb S, Pretorius C, Goba P (2001) Hydrological systems modelling research programme: hydrological processes. WRC Report No. 637/1/01. Water Research Commission, Pretoria, South Africa. 102 pp.

Marui A, Yasuhara M, Kuroda K, Takayama S (1993) Subsurface water movement and transmission of rainwater pressure through a clay layer. *Proceedings of the Yokohama*

Symposium, on the Hydrology of Warm Humid Regions, IAHS Publication No. 216: 463-470.

McWhorter DB, Sunada DK (1977) *Ground-water hydrology and hydraulics*. Water Resources Publication.

Miyazaki T, Ibrahimi MK, Nishimura T (2012) Shallow groundwater dynamics controlled by Lisse and reverse Wieringermeer effects. *Journal of Sustainable Watershed Science and Management* 1, No. 2: 36-45.

Novakowski KS, Gillham RW (1988) Field investigations of the nature of water-table response to precipitation in shallow water-table environments. *Journal of Hydrology* 97, No. 1: 23-32.

Rosenberry DO, Winter TC (1997) Dynamics of water-table fluctuations in an upland between two prairie-pothole wetlands in North Dakota. *Journal of Hydrology* 191, No. 1: 266-289.

Waswa GW (2013) Transient pressure waves in hillslopes. PhD Thesis, Scholl of Engineering, KwaZulu-Natal, Durban, Soiuth Africa. 120.

Waswa GW, Lorentz SA (2015a) Transmission of pressure head through the zone of tension saturation in the Lisse effect phenomenon. *Hydrological Sciences Journal* 61, No. 10: 1770-1777.

Waswa GW, Lorentz SA (2015b) Energy considerations in groundwater-ridging mechanism of streamflow generation. *Hydrological Processes* 29, No. 23: 4932-4946

Waswa GW, Clulow AD, Freese C, Le Roux PA, Lorentz SA (2013) Transient pressure waves through vadose zone and rapid water table response. *Vadose Zone Journal* 12, No. 1: 1048–1060.

Weeks EP (2002) The Lisse Effect revisited. *Groundwater* 40, No. 6: 652-656.

Zang YG, Sun DM, Feng P, Semprich S (2017) Numerical analysis of groundwater ridging processes considering water air-flow in a hillslope. *Groundwater*. Doi: 10.1111/gwat.12602.

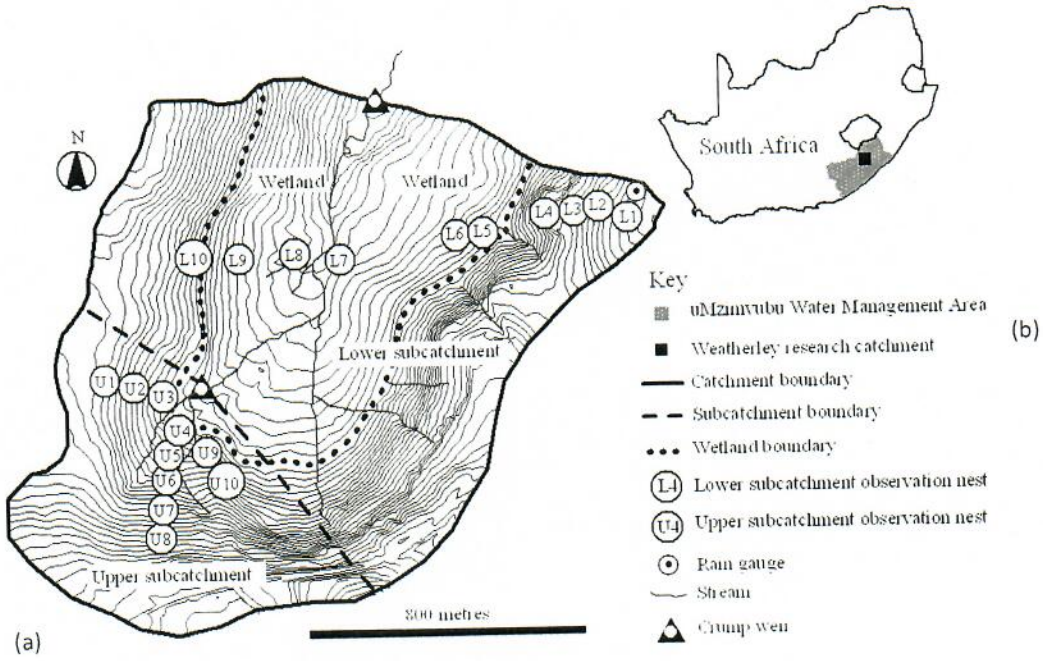

Figure 1. Study site (adopted from Lorentz *et al.*, 2001), (a) Weatherley research catchment and (b) its location in South Africa.

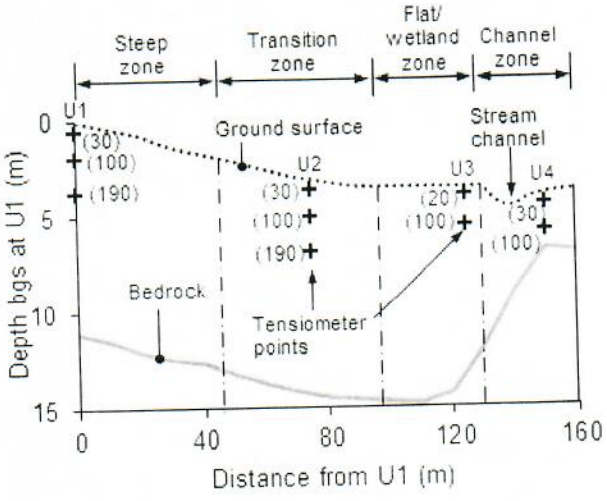

Figure 2: A transect showing the positions of tensiometers (the values in parenthesis are depth in cm below ground surface at the respective nests). The Depth below ground surface (bgs) at U1 is exaggerated two times.

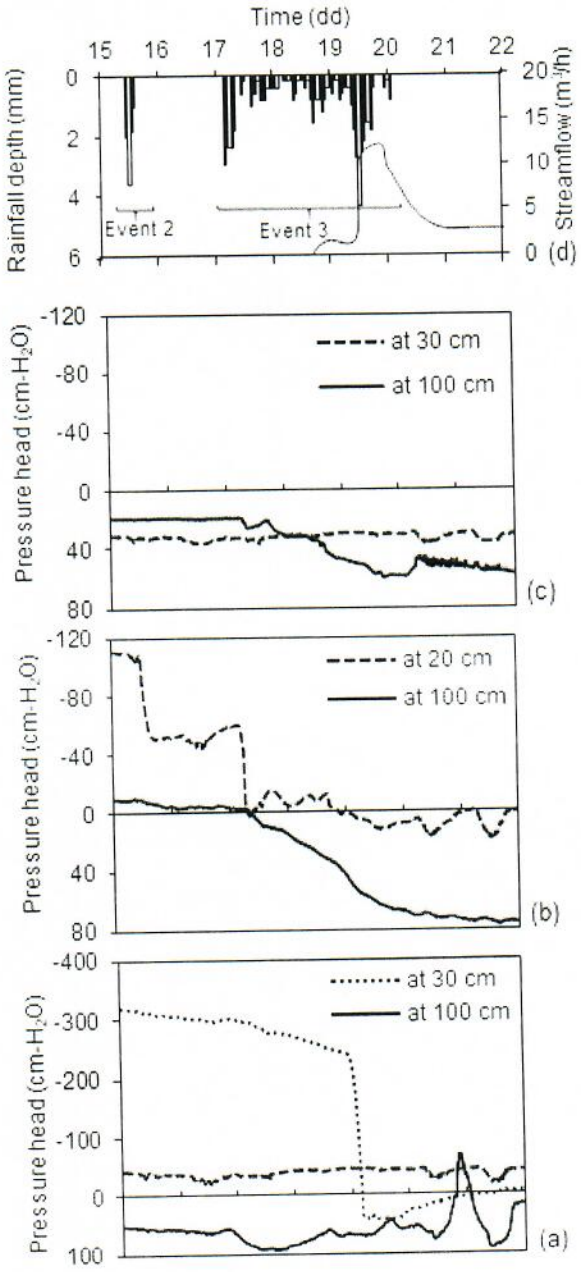

Figure 3: Pore-water pressure head responses at observations point (a) U2, (b) U3 and (c) U4, and (d) stream flow response to (d) rainfall Events 2 and 3.

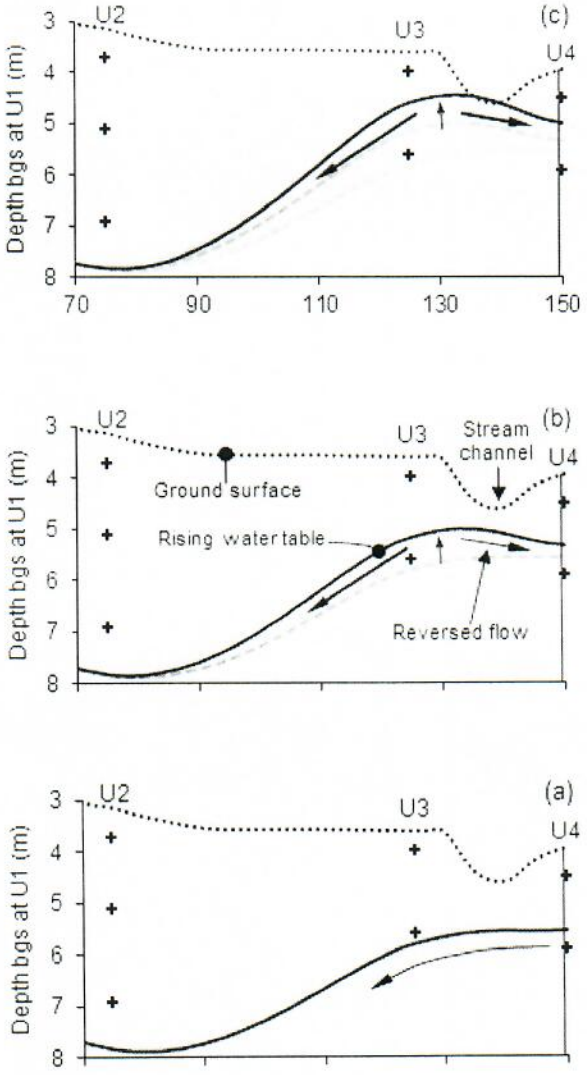

Figure 4: Water table configurations at the study site (a) prior to rainfall Event 2: 15th September 2000 at 00:00H; (b) during rainfall Event 3 on 18th September 2000 at 00:00H; and (c) during Event 3 on 19th September at 00:00H. The Depth below ground surface (bgs) at U1 is exaggerated two times.

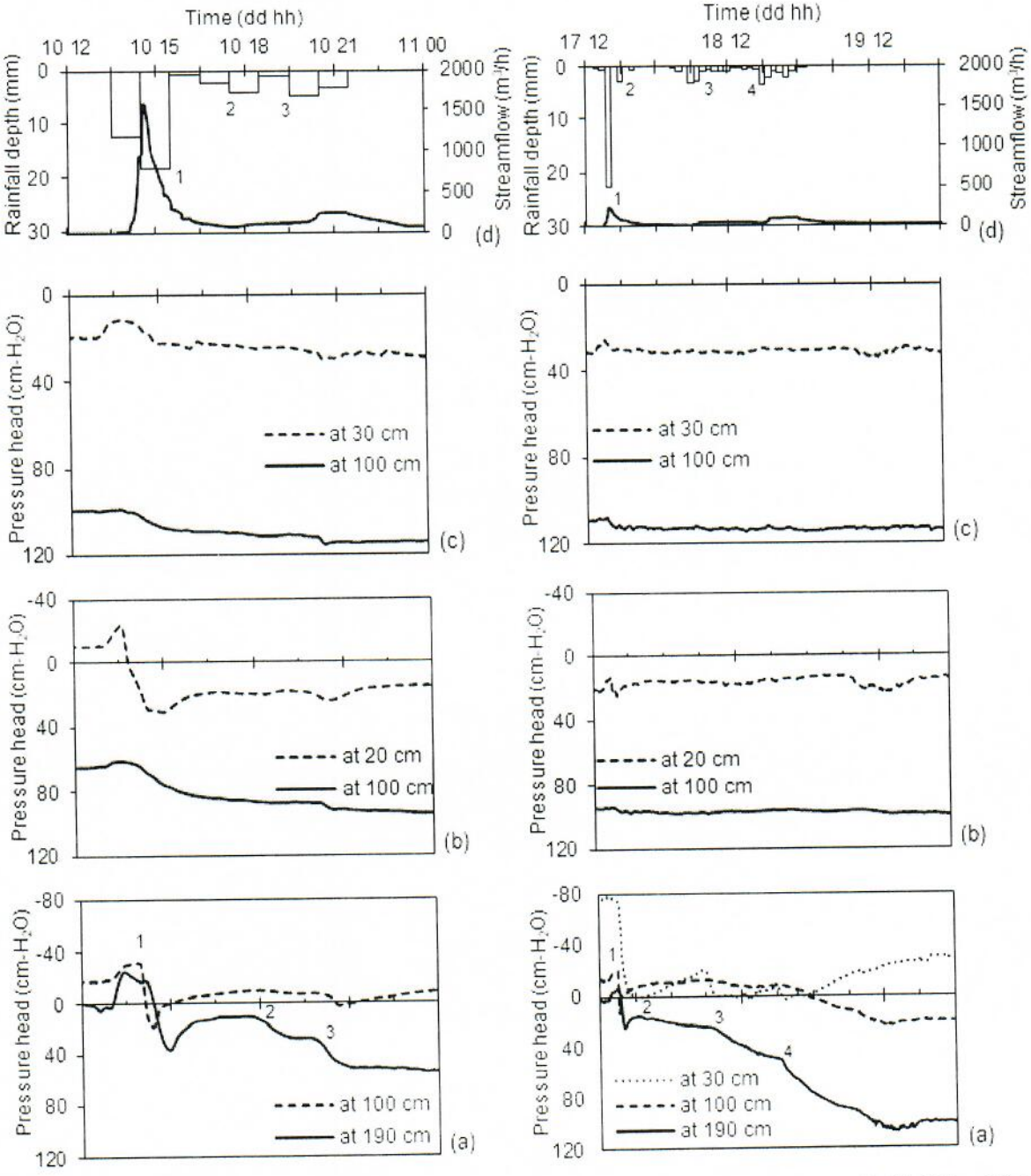

Figure 5 (*left column*): Pore-water pressure head responses at observations nest (a) U2, (b) U3 and (c) U4, and (d) stream flow response to (d) rainfall Event 70 [10th – 11th March]

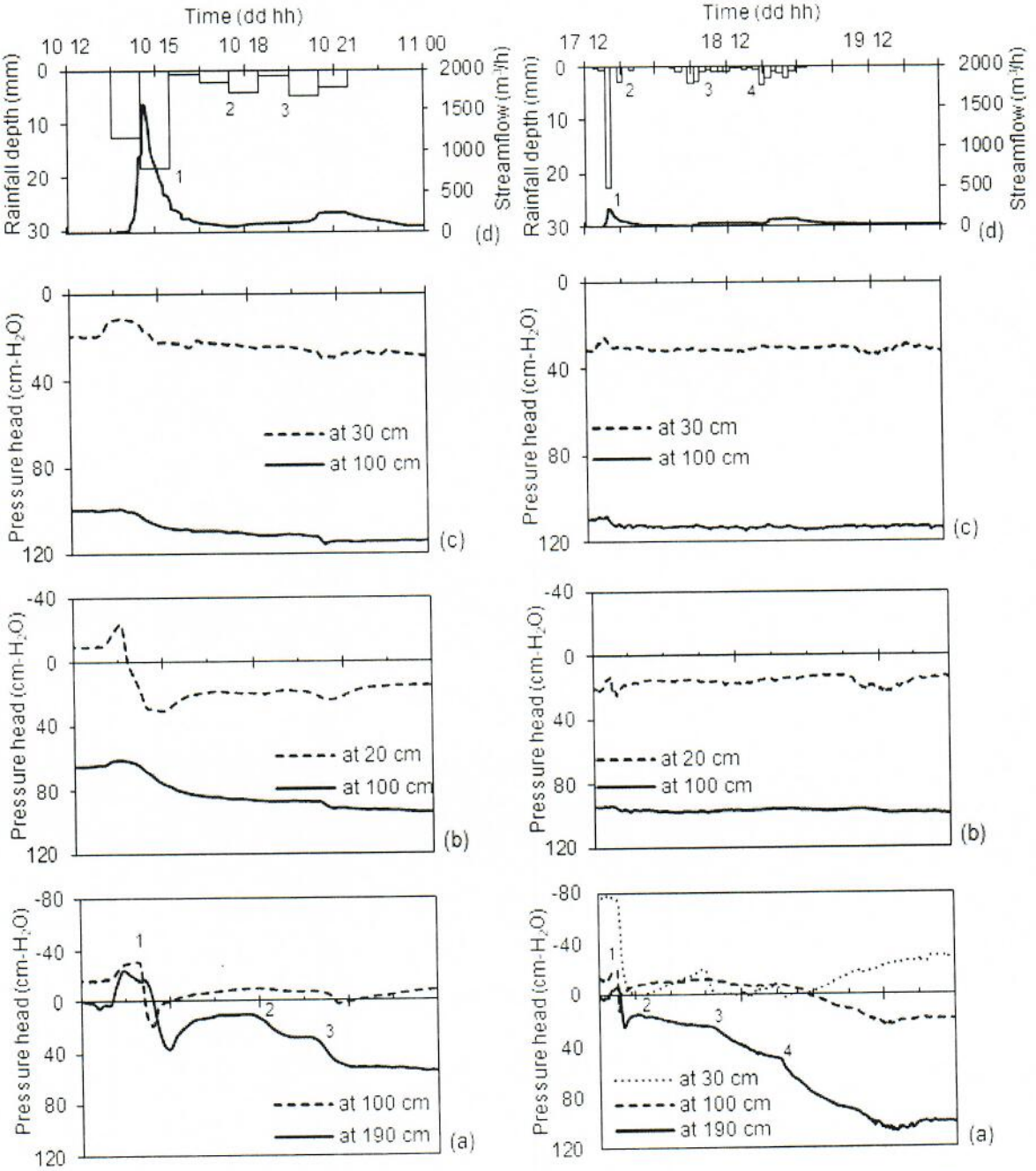

Figure 6 (*right column*): Pore-water pressure head responses at observations nest (a) U2, (b) U3 and (c) U4, and (d) stream flow response to (d) rainfall Event 75 [17TH – 19TH March 2001]

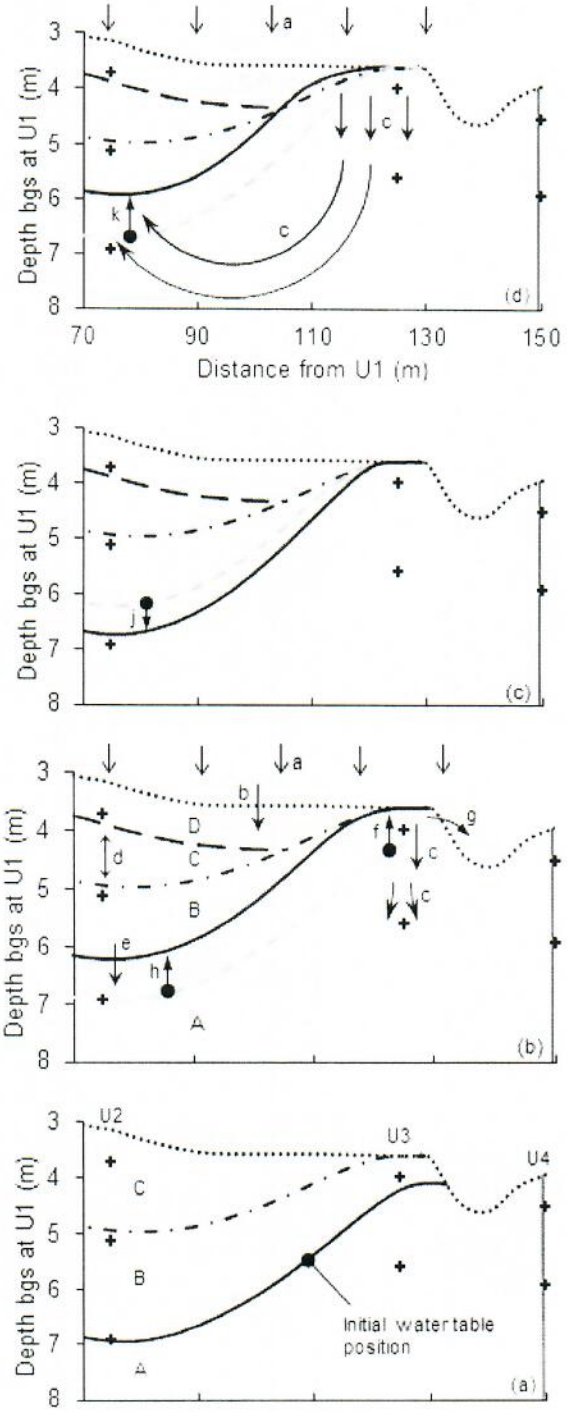

Figure 7: A model of groundwater ridging and the Lisse effect on groundwater flow at the wetland zone in the weatherly Research Catchment, South Africa: (a) the initial water table with capillary fringe extended to ground surface at U3, (b) the Lisse effect type rapid water table response at U2 and the groundwater ridging rapid water table response at U3, (c) the receding water table at U2 due to dissipation of entrapped pressurised pore air, (d) Intense rainfall induced pressure head and their upwelling at U2, causing an increase in pressure head at U2. The Depth below ground surface (bgs) at U1 is exaggerated two times.

Groundwater Zones: A: Phreatic zone; B: the tension saturation/near saturation zone; C: Unsaturated zone with continuous pore air; D: Infiltration profile.

Key to arrows: *a*: intense rainfall (e.g. Event 70); *b*: infiltration in the unsaturated zone; *c*: intense rainfall-induced pressure head; *d*: compressed pore air between the wetting front and the top boundary of the capillary fringe (zone B); *e*: pressurised pore air-induced pressure head; *f*: rising water table due to intense-rainfall induced pressure head; *g*: gravity flow of groundwater into the stream channel from the converted capillary fringe; *h*: the Lisse effect water table rise; *j*: falling water table due to dissipation of pressurized pore air; *k*: rising water table (pressure head) at U2 due to upwelling of intense rainfall induced pressure head.

Table 1: Characteristics of the rainfall events

Event No	Date	Duration (hours)	Amount (mm)	Average intensity (mm/h)	12-min max intensity (mm/h)
3	17–20.09.00	81	49.8	0.6	7
70	10 Mar	7	47.2	6.7	75
75	17 Mar	5	26.6	5.3	89
76	18-19 Mar	21	24.8	1.8	10